1.3-W Ripple-Free Superluminescent Diode

L. Burrow, F. Causa, *Member, IEEE*, and J. Sarma

***Abstract*—This letter presents the experimental characterization of tapered and stripe superluminescent diodes fabricated from 980-nm high-power triple quantum-well InGaAs–AlGaAs semiconductor material. Record output powers in excess of 1.3 W pulsed have been measured, with 0.1-dB spectral modulation and maximum wall-plug efficiency 16%. Almost 1-W optical power into multimode optical fibers has been achieved with preliminary measurements of coupling efficiency.**

***Index Terms*—Optoelectronic devices, semiconductor device modeling, superluminescent diodes (SLDs).**

I. Introduction

SUPER-LUMINESCENT diodes (SLDs) are high-power semiconductor optical sources with relatively broad spectral linewidth increasingly used for a variety of applications including optical coherence tomography, wavelength-division-multiplexing systems, fiber-optic gyroscopes, and short-haul communications. The basic crucial device feature needed to achieve high-power SLD operation is low facet reflectivity to prevent lasing even at the required high pumping levels. An unpumped, absorbing region, e.g., [1], at the rear end of the SLD is a commonly used method to reduce facet reflectivity. However, the drawback of this simple straightforward method is that the unpumped absorber becomes progressively transparent because of optical pumping and, therefore, ineffective especially for high-power operation unless impractically long device sections are used. Antireflection (AR) facet coating [2] is an alternative technique of reducing facet reflectivity, but in this case the inconvenience is that expensive multilayer AR coatings have to be designed to drastically reduce facet reflectivity. Tilting [3], or bending [4] the injection contact with respect to the output facet may be effective for reducing optical feedback, but the undesired effect here is that spatial output field profile is asymmetric, thereby reducing coupling efficiency. On the other hand, the etched deflector introduced in [5] is a simple and inexpensive method for effectively reducing the rear facet reflectivity even for high-power operation. In [5], the rear deflector was fabricated by chemical etching resulting in a V-groove at 10° to the $(01\bar{1})$ plane, through the active layer. In this letter, the deflector is ion beam etched at 45° to the $(01\bar{1})$ plane making the oscillation suppression even more efficient. Importantly, low facet reflectivities are also essential to reduce the SLD output spectrum modulation (Fabry–Pérot resonances due to residual facet reflectivity) and achieve the desired ripple-free output spectrum.

This letter presents the experimental characterization of tapered and stripe SLDs fabricated from 980-nm high-power semiconductor material. The experimental results have been interpreted using theoretical models developed in-house [6].

TABLE I
LARGE OPTICAL CAVITY TRIPLE-QUANTUM-WELL MATERIAL EPITAXY

Layer	Thickness (μm)	Composition	Doping	Dopant
Cap	0.2	GaAs	$1\ 10^{19}$	Zn
Cladding	1.4	$Al_{0.44}Ga_{0.56}As$	$1\ 10^{18}$	C
Guide	0.6	$Al_{0.3}Ga_{0.7}As$	$3\ 10^{16}$	C
Barrier	100Å	GaAs		
QW	70Å	$In_{0.2}Ga_{0.8}As$		
Barrier	100Å	GaAs		
QW	70Å	$In_{0.2}Ga_{0.8}As$		
Barrier	100Å	GaAs		
QW	70Å	$In_{0.2}Ga_{0.8}As$		
Barrier	100Å	GaAs		
Guide	0.6	$Al_{0.3}Ga_{0.7}As$	$3\ 10^{16}$	Si
Cladding	1.4	$Al_{0.44}Ga_{0.56}As$	$1.4\ 10^{18}$	Si
Buffer	0.5	GaAs	$1\ 10^{18}$	Si

II. Device Structure

Straight stripe SLDs (SS-SLDs) and tapered SLDs (T-SLDs) were fabricated from a specially designed metal–organic vapor phase epitaxy-grown high-power large optical cavity strained InGaAs–GaAs–AlGaAs double heterostructure material with three 7-nm quantum wells (QWs) surrounded by 10-nm GaAs barriers (Table I). The ion beam etched ridge for current injection is shallow (no change in lateral effective refractive index) but sufficient to reduce current spreading. The V-groove deflector has been ion beam etched at 45° with respect to the output facet, at a distance of 200 μm from the rear of the active region. The output facet is AR-coated with a single layer of ZrO_2–TiO_2, which reduces the facet reflectivity to 1%. The AR-coating on the output facet increases facet transmission, but more importantly, decreases gain saturation at the rear of the active region by significantly reducing optical feedback. Two types of devices are considered in this letter: The first type is the SS-SLD characterized by a stripe injection contact (Fig. 1) while the second type of device is the T-SLD with a tapered (triangular) metal injection contact.

The devices were mounted n-side-down onto copper heat sinks using conductive silver loaded epoxy resin. The p-side was contacted with gold wire using a thermocompression ultrasonic bonder. Several SS-SLDs (100 μm width, 1 mm length) and T-SLDs (200 μm width, 1 mm length), with the same active volume but different geometry, were fabricated and characterized to compare performance.

III. Experimental and Theoretical Results

The light–current (*L–I*) curves of Fig. 2 were measured from devices operating under pulsed conditions (5 μs, 200 Hz). As typically observed for SLDs, the *L–I* curves of Fig. 2 are linear in

Manuscript received December 15, 2004; revised May 19, 2005.

The authors are with the Department of Electronic and Electrical Engineering, University of Bath, Bath BA2 7AY, U.K. (e-mail: f.causa@bath.ac.uk).

Digital Object Identifier 10.1109/LPT.2005.853027

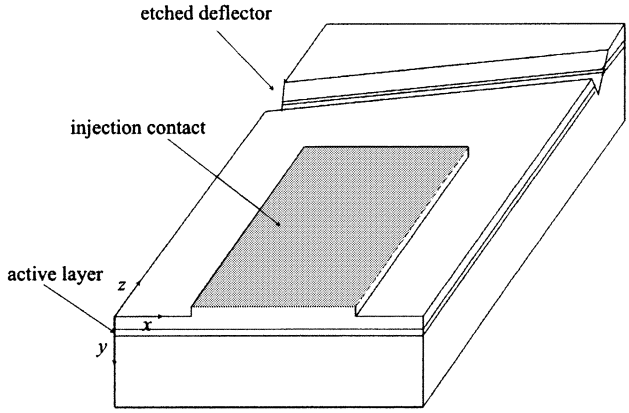

Fig. 1. Schematic of SS-SLD device geometry—the dark gray area represents the metal injection contact.

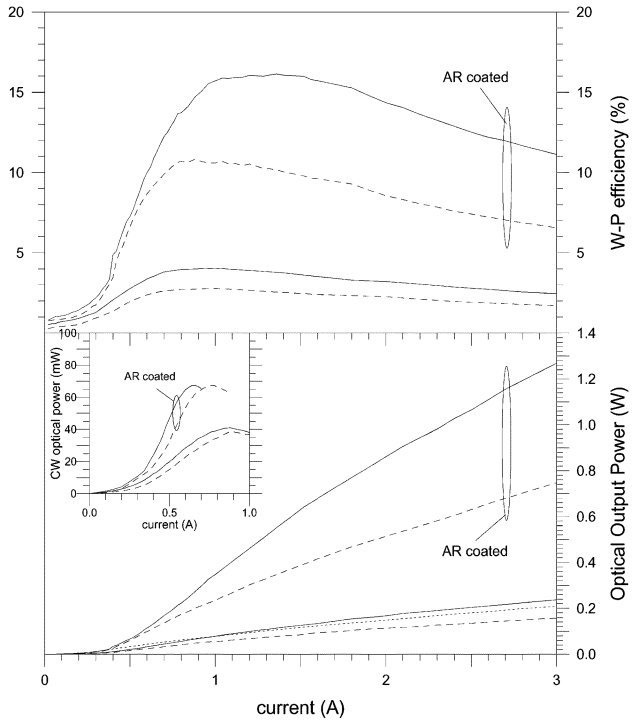

Fig. 2. *L–I* characteristic and W-P efficiency measured from in-house fabricated SS-SLDs (dashed lines) and T-SLDs (continuous lines) before and after AR-coating. The *L–I* curve measured from T-SLDs with $W = 100\,\mu$m and $L = 1$ mm (dotted line) is also included for completeness. *L–I* characteristics measured from SS-SLDs (dashed line) and T-SLDs (continuous line) under CW operation before and after AR-coating are shown in the inset.

the spontaneous emission regime (nonpositive optical gain), becoming superlinear at the on-set of superluminescence (amplified spontaneous emission (ASE) regime, positive optical gain) and then sublinear when gain saturation occurs. As expected T-SLDs are more efficient than SS-SLDs since the optical gain saturation due to the optical feedback is reduced with a tapered geometry injection metal contact, [3], [5]. In tapered devices, most of the optical feedback is dissipated in the lossy region around the gain region under the metal contact. This effect is noticeable when comparing the output optical power measured from SS-SLDs and T-SLDs of either same active volume (that is, the same injection contact surface area) or the same width and length (in which case, the T-SLD active volume is half that of the SS-SLD). In both cases, the optical output power measured from T-SLD is higher than that measured from SS-SLDs (Fig. 2).

Optical output powers in excess of 1.3 W were measured at 3 A from AR-coated T-SLDs, the highest SLD output power presented in the literature to the best of our knowledge, with 16% maximum wall-plug (W-P) efficiency. With respect to uncoated T-SLDs, the output power measured from the AR-coated devices presents a factor of five increase in output power and W-P with a corresponding shift and flattening of the W-P peak at higher currents. The optical power saturation point was estimated from the change of slope efficiency against input current. As expected, it was found that the optical power saturation point changes before and after AR-coating, obtaining 0.6 and 0.8 A, respectively, for SS-SLDs and 0.8 and 1.5 A, respectively, for T-SLDs, indicating that T-SLDs are more efficient than SS-SLDs.

Notwithstanding the poor thermal-sinking, the SLDs described in this letter were tested also under continuous-wave (CW) operation achieving optical output powers in excess of 67 mW at 600 mA from AR-coated T-SLDs, an improvement of 64%–70% with respect to corresponding non-AR-coated devices (inset of Fig. 2). Thermal rollover is observed at the maximum CW optical power level achieved (67 mW), corresponding to 600- and 850-mA input current for AR-T-SLDs and AR-SS-SLDs, respectively. The results presented in the inset of Fig. 2 indicate that maximum CW output power is limited by the thermal properties of the semiconductor material used to fabricate the SLDs (corresponding to approximately 2-MW $\cdot$ cm^{-2} internal power density at the facet). However, it is noticed that also under CW operation the T-SLD is more efficient than the SS-SLD.

The far-field intensity profiles and corresponding spectral characteristics measured at different currents from T-SLDs and SS-SLDs are presented in Fig. 3. The broad far field typical of spontaneous emission at low currents reduces to the typical bell-shaped characteristic of ASE, with output beam full-width at half-maximum (FWHM) of 37° for SS-SLDs and 43° for T-SLDs. After the onset of optical gain saturation ($I \sim 1.5$ A), the FWHM beam width increases slightly $<10\%$. The theoretical far fields computed with ray model [6] have also been included for comparison. As expected, the far fields measured from SS-SLDs have the characteristic "triangular" profile, while those measured from T-SLDs have a "flat-top" profile rounded because of current spreading and carrier diffusion effects [6]. The FWHM of the vertical far-field intensity profile is 35° in both cases.

Spectral measurements were taken using an optical spectrum analyzer (OSA) with 0.1-nm resolution. The spectral characteristics from T-SLDs and SS-SLDs are similar with 18-nm FWHM spectral width (Fig. 3). The corresponding coherence length is $L_c = 0.66(\lambda^2/\Delta\lambda) \cong 35\ \mu$m. Up to the highest currents of interest here ($I = 3A$, or current density $J = 3$ kA $\cdot$ cm^{-2}) the measured output spectrum present intensity fluctuation, comparing well with other published results, e.g., [4] (inset of Fig. 3). The mode spacing was estimated from the measured spectrum to be 0.1 nm, in agreement with the 0.119-nm theoretical estimate. The spectral modulation becomes less pronounced after AR-coating. The coherence curves obtained for SS-SLDs, T-SLDs, and AR-T-SLDs are

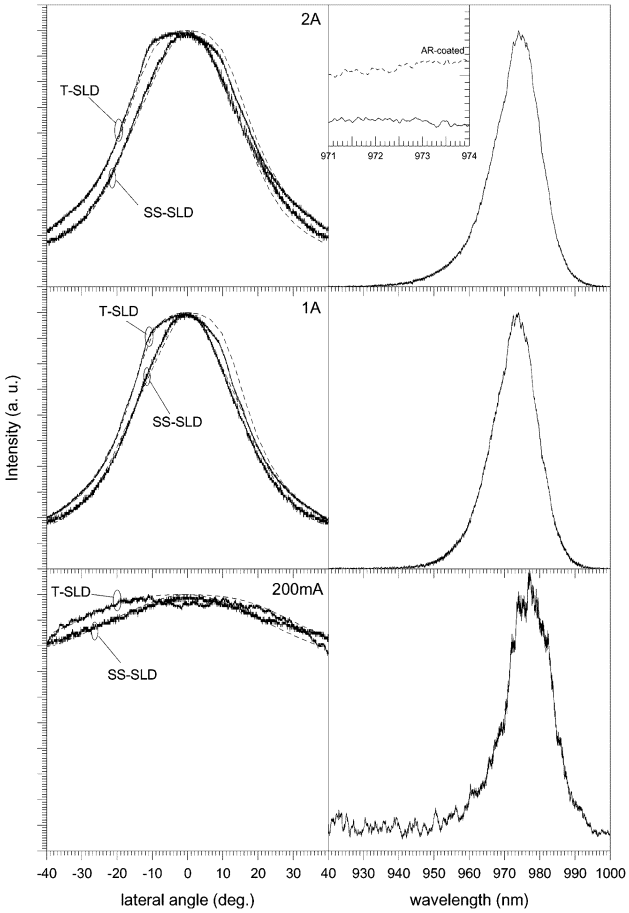

Fig. 3. Measured (solid line) and theoretical (dashed line) SS-SLDs and T-SLDs far-field intensity profiles at different injection currents and corresponding spectral characteristics (resolution 0.1 nm). The spectral modulation before and after AR-coating is presented in detail in the inset (resolution 0.01 nm).

compared in Fig. 4. Qualitatively, it is noticed that the coherence curve for AR-T-SLDs has less pronounced secondary subpeaks with respect to that of non-AR-coated T-SLDs. In particular, a secondary subpeak due to residual Fabry–Pérot modulations is visible at a distance of 3.39 mm, corresponding to an effective refractive index for the vertical (TE) optical mode of $n_m \sim 3.39$, in agreement with the theoretical estimate $n_m = 3.3205$ for the given epitaxy.

Coupling efficiencies of 75% have been measured by butt-coupling the SLDs to multimode plastic optical fibers (POF) ($NA = 0.39, 400$ μm core diameter) using an index-matching gel. This corresponds to 975 mW of optical power coupled into POFs making the SLDs described in this letter useful for applications such as optical communications, e.g., [7], where SLDs emitting at 1.5 μm have been used for wavelength multiplexing, and sensing, for example in optical coherence tomography, e.g., [8], where SLDs emitting at 980 nm (28 nm spectral linewidth) are typically used.

IV. Conclusion

The experimental characterization of tapered and stripe geometry SLDs has been presented. Record-breaking output powers in excess of 1.3 W pulsed (67-nm CW at 600 mA) have been measured from AR-coated T-SLDs, with 16% peak W-P efficiency and ripple-free output spectrum (0.1-dB spectral modulation). The radiation patterns measured under ASE operation are well represented by a cosine profile to the power $n \sim 12$. Preliminary coupling efficiency measurements into POFs have shown that it is possible to achieve $\sim$1-W power into the fiber.

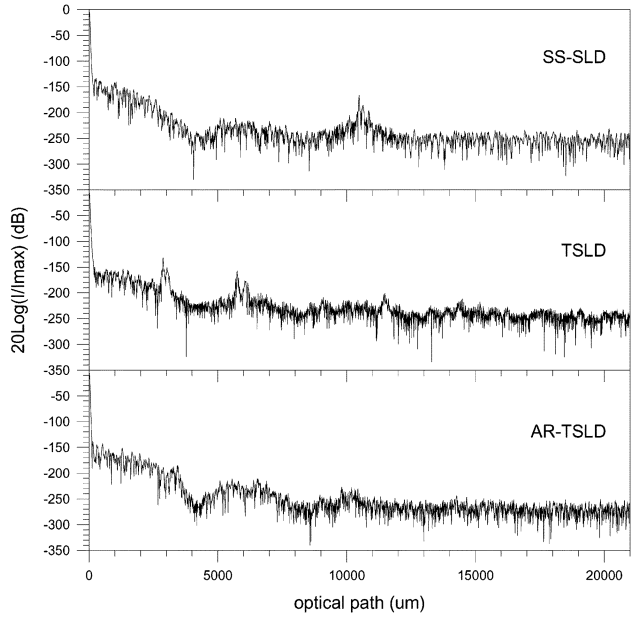

Fig. 4. Coherence curves for SS-SLDs, T-SLDs, and AR-T-SLDs.

Acknowledgment

The authors would like to acknowledge Dr. J. S. Roberts (EPSRC National Centre for III-V Technologies, University of Sheffield, U.K.), for providing the semiconductor material and T. J. Ryan (University of Bath, U.K.), for advice on device fabrication.

References

[1] I. M. Joindot and C. Y. Boisrobert, "Peculiar features of InGaAsP DH superluminescent diodes," *IEEE J. Quantum Electron.*, vol. 25, no. 7, pp. 1659–1665, Jul. 1989.

[2] I. P. Kaminow, G. Eisenstein, L. W. Stultz, and A. G. Dentai, "Lateral confinement InGaAsP superluminescent diode at 1.3 microns," *IEEE J. Quantum Electron.*, vol. 19, no. 1, pp. 78–82, Jan. 1983.

[3] T. Yamatoya, S. Mori, F. Koyama, and K. Iga, "High power GaInAsP/InP strained quantum well superluminescent diode with tapered active region," *Jpn. J. Appl. Phys.*, vol. 38, no. 9A, p. 5121, Sep. 1999.

[4] L. Fu, H. Schweizer, Y. Zhang, L. Li, A. M. Baechle, S. Jochum, G. C. Bernatz, and S. Hansmann, "Design and realization of high-power ripple-free superluminescent diodes at 1300 nm," *IEEE J. Quantum Electron.*, vol. 40, no. 9, pp. 1270–1274, Sep. 2004.

[5] I. Middlemast, J. Sarma, and S. Yunus, "High power tapered superluminescent diodes using novel etched deflectors," *Electron. Lett.*, vol. 33, no. 10, pp. 903–904, May. 997.

[6] F. Causa and J. Sarma, "A realistic model for the output beam profile of stripe and tapered superluminescent LEDs," *Appl. Opt.*, vol. 42, no. 21, pp. 4341–4348, Jul. 2003.

[7] F. Koyama, "High power superluminescent diodes for multi-wavelength light source," in *IEEE LEOS Annu. Meeting*, 1997, Paper TuY2, pp. 333–334.

[8] A. V. Zvyagin, K. K. M. B. Dilusha Silva, S. A. Alexandrov, T. R. Hillman, J. J. Armstrong, T. Tsuzuki, and D. D. Sampson, "Refractive index tomography of turbid media by bifocal optical coherence refractometry," *Opt. Express*, vol. 11, no. 25, pp. 3503–3517, Dec. 15, 2003.